Magnetostriction of rare-earth random magnetic anisotropy spin glasses

A. del Moral and J. I. Arnaudas
Laboratorio Magnetismo de Sólidos, Instituto de Ciencia de Materiales de Aragón (ICMA) and Departamento de Física de la Materia Condensada, Universidad de Zaragoza and Consejo Superior de Investigaciones Científicas (CSIC), 50009-Zaragoza, Spain
(Received 2 May 1988)

A model of magnetostriction for single-ion random magnetic anisotropy (RMA) spin glasses (SG) is developed, the calculation being based on the replica technique. An overall uniform strain is assumed and coupled to the local easy axis (or easy plane) by an adequate projection. The obtained bulk magnetostriction becomes proportional to the average quadrupolar moment, which depends upon the assumed ferromagnetic uniform exchange, J_0, and the RMA crystal field (CEF), D_0, strengths. Magnetostriction measurements parallel ($\lambda_\parallel$) and perpendicular ($\lambda_\perp$) to the applied magnetic field (up to 7 T) have been performed between 4.2 and 150 K (much larger than the SG temperature, T_{SG}) for the amorphous spin glasses $R_{40}Y_{23}Cu_{37}$ (R =Tb, Dy, Ho, and Er). Anisotropic magnetostriction is a forced effect, with no sign of saturation, and is quite large well above T_{SG}. The developed model fits quantitatively and remarkably well the temperature variation of the anisotropic magnetostriction, $\lambda_t=\lambda_\parallel-\lambda_\perp$, in the case of Tb, Dy, and Ho alloys. The values obtained from the fit for D_0, respectively, are +3.0, +1.25, and +0.6 K. For Er, D_0 becomes −0.37 K. The signs of D_0 are in agreement with having local axial anisotropy for the Tb, Dy, and Ho compounds, and planar for the Er one, in good agreement with the signs of the α_J Stevens quadrupolar parameter. From the above comparison between our theory and the measured magnetostriction, values for M_2/C_e, where M_2 is the magnetoelastic coupling coefficient and C_e the average elastic constant, are also obtained, being in the relation +1:+0.31:+0.18:−0.28, in remarkably good agreement with the point-charge model of CEF especially developed for those amorphous alloys.

I. INTRODUCTION

Random magnetic anisotropy (RMA) magnetism is a subject of steadily growing interest.[1–10] In this paper we report magnetostriction measurements on random magnetic anisotropy spin glasses (SG) of amorphous structure together with a model of magnetoelastic coupling in those systems, which renders a good quantitative explanation of the experimental findings. Amorphous rare earth (R) alloys are materials expected to present RMA with random local easy axis, due to the evironmental disorder. The origin of the RMA must be associated with the electric field gradient acting upon the R^{+3} quadrupolar ionic charge distribution. Such RMA is naturally expected to produce a spin-glass freezing of the spin directions of equal nature of the one well observed in random exchange spin glasses.

Let us now briefly summarize the main findings in RMA spin glasses from the theoretical point of view, in order to ascertain whether amorphous alloys $R_{40}Y_{23}Cu_{37}$ (R =Tb, Dy, Ho, and Er), which are the object of our study, are true RMA spin glasses. A full and detailed account of magnetic properties of amorphous $R_{40}Y_{23}Cu_{37}$ alloys will be given elsewhere.[11] A finger print of RMA magnets is the absence of ferromagnetic long-range order in the presence of ferromagnetic exchange. Imry and Ma,[12] and Aharony and Pytte,[13] found that no matter how weak RMA is, it will destroy the long-range order. Besides, the initial susceptibility, $\chi_0\equiv(M/H)_{H\to 0}$, should diverge at $T\le T_{SG}$ (Ref. 13) or become very large if J_0/D_0 is not too small [$\chi_0\approx(J_0/D_0)^4$], according to recent calculations of Chudnovsky *et al.*[14] In fact, as in the random exchange SG case, the spin freezing at T_{SG} will produce the display of acute cusps of the initial susceptibility. A RMA system should also exhibit a finite coercitivity and hysteretic behavior, as shown by Callen *et al.*[15] and Patterson *et al.*[16] On top of all that, one should expect strong magnetic aftereffects at remanence. All this means that T_{SG} represents the start of strong irreversibilities. All these predictions have been observed in the present a-$R_{40}Y_{23}Cu_{37}$ alloys. The initial ac susceptibility presents acute cusps at T_{SG} (Ref. 17) (see Table I), and besides, the paramagnetic Curie temperature Θ is positive, indicating the presence of positive exchange interactions. Besides the magnetization at relatively low fields ($\approx$1 T) shows broad cusps around T_{SG}. Arrott plots of M^2 versus H/M show the inexistence of spontaneous magnetization and the approaching of H/M to the demagnetizing field values for $T\le T_{SG}$ and low magnetizations. We also observed strong remanence and coercitivity below T_{SG}, and a magnetic aftereffect at remanence, that, for long enough time, was of the form $\ln t$. We then conclude that, in the case of amorphous $R_{40}Y_{23}Cu_{37}$ alloys, we are, in fact, in the presence of RMA spin glasses.

The organization of the paper is as follows. In Sec. II A we outline the main steps of the theory of RMA magnets, with specialization to our present systems. In Sec. II B we develop a model of magnetostriction in RMA spin glasses, either with local axial or planar an-

TABLE I. Spin-glass temperature, T_{SG}; exchange paramagnetic Curie temperature, Θ; random CEF strength parameter, D_0, and M_2/C_e, with M_2, the magnetoelastic coupling parameter, and C_e the average elastic stiffness constant, deduced for the amorphous $R_{40}Y_{23}Cu_{37}$ alloys by comparison between experiments (Sec. III) and proposed model (Sec. II).

Alloy	$T_{SG}(K)$ [a]	$\Theta(K)$	$D_0(K)$	(M_2/C_e) $(\times 10^{-6})$
$Tb_{40}Y_{23}Cu_{37}$	36	7.5	+3.0	+29.2
$Dy_{40}Y_{23}Cu_{37}$	23.5	4.0	+1.25	+9.2
$Ho_{40}Y_{23}Cu_{37}$	12.6	1.3	+0.60	+4.4
$Er_{40}Y_{23}Cu_{37}$	7	$\simeq 0$	−0.37	−8.3[b]

[a]From Ref. 17.
[b]For Er ion this value corresponds to $M_2^{\perp}/C_e$ (see Sec. II B 2).

isotropy. The magnetostrictive bulk strain is calculated in Sec. II C. In Sec. III we present the experimental results of magnetostriction in a-$R_{40}Y_{23}Cu_{37}$ alloys, and in Sec. IV we make a quantitative comparison of the model with experiment. Finally, in Sec. V we extract the conclusions of our work.

II. MODEL OF MAGNETOSTRICTION IN RMA SPIN GLASSES

A. Outline of theory of RMA magnets

The theory of RMA magnets is by now reasonably well established since the pioneering work of Harris *et al.*,[1] Aharony,[18] and Chen and Lubensky,[19] as already mentioned. In the following we review and closely adhere to the early model developed by Aharony,[18] although we will work in the discrete lattice approximation instead of the continuous one used in renormalization-group calculations. The model quoted here is paramount for the development of the magnetoelastic coupling model proposed in Sec. II B. One starts from the Hamiltonian

$$H=-\sum_{\mathbf{x},\boldsymbol{\delta}} J(\mathbf{x},\mathbf{x}+\boldsymbol{\delta})\mathbf{S}(\mathbf{x})\cdot\mathbf{S}(\mathbf{x}+\boldsymbol{\delta}) - D_0\sum_{\mathbf{x}}[\hat{\mathbf{a}}(\mathbf{x})\cdot\mathbf{S}(\mathbf{x})]^2 , \tag{2.1}$$

where $\mathbf{S}(\mathbf{x})$ is a m-component spin vector, located at the site $\mathbf{x}$ of a d-dimensional amorphous (or also crystalline) lattice ($\boldsymbol{\delta}$ is a vector connecting site $\mathbf{x}$ with the average z NN); $J(\mathbf{x},\mathbf{x}+\boldsymbol{\delta})$ is the exchange interaction strength, and $\hat{\mathbf{a}}(\mathbf{x})$ is a unit vector pointing in the local (random) direction of the uniaxial anisotropy at site $\mathbf{x}$. As said before, this anisotropy arises from the interaction of the gradient of the crystalline electric field (CEF) with the quadrupolar moment of the charge distribution of the rare-earth ion. We have assumed that the random nature of the amorphous lattice causes the local easy direction to vary randomly, but we have ignored possible fluctuations in the strength of the local anisotropy by making D_0 a constant. Experiments performed on rare-earth amorphous alloys show that this is in fact the case.[20,21]

In order to evaluate the free energy of the system, one defines the partition function, namely,

$$Z\{\hat{\mathbf{a}}(\mathbf{x})\}=\mathrm{Tr}[\exp(-\beta H)] , \tag{2.2}$$

where the trace is taken over the m-dimensional spin space, ($\beta\equiv 1/k_BT$). As usual, we assume a quenched system and therefore average over the free energies of all possible random configurations of directions $\{\hat{\mathbf{a}}(\mathbf{x})\}$, merely

$$F=-\frac{1}{\beta}\sum_{\mathbf{x}}\int d^m\hat{\mathbf{a}}(\mathbf{x})P\{\hat{\mathbf{a}}(\mathbf{x})\}\ln Z\{\hat{\mathbf{a}}(\mathbf{x})\} , \tag{2.3}$$

where $P\{\hat{\mathbf{a}}(\mathbf{x})\}$ is the probability of finding a configuration of directions $\{\hat{\mathbf{a}}(\mathbf{x})\}$, and the integral is performed over the m-dimensional sphere. We use now the usual replica trick, making

$$\ln Z\{\hat{\mathbf{a}}(\mathbf{x})\}=\lim_{n\to 0}\frac{Z^n-1}{n} . \tag{2.4}$$

Substitution of (2.4) in Eq. (2.3) gives

$$-\beta F=\lim_{n\to 0}\frac{1}{n}(\mathrm{Tr}_n e^{-\beta H_{\mathrm{eff}}}-1) , \tag{2.5}$$

where Tr_n is the trace over the n-replicated spin system, and where the effective Hamiltonian has the form

$$H_{\mathrm{eff}}=-J_0\sum_{(\mathbf{x},\boldsymbol{\delta},\alpha)}\mathbf{S}^{\alpha}(\mathbf{x})\cdot\mathbf{S}^{\alpha}(\mathbf{x}+\boldsymbol{\delta})-G\{\sigma(\mathbf{x})\} , \tag{2.6}$$

where we have assumed that the exchange interaction is uniform.

$$\sigma\equiv(\mathbf{S}_1,\ldots,\mathbf{S}_n)=(S_{11},\ldots,S_{1m},S_{21},\ldots,S_{nm})$$

is a generalized spin in the spin replica space of dimension nm, and α stands for the replica index. Besides,

$$e^{-G\{\sigma\}}=\int d^m\hat{\mathbf{a}}(\mathbf{x})P\{\hat{\mathbf{a}}(\mathbf{x})\} \times\exp\left[D_0\sum_{\mathbf{x}}\sum_{\alpha=1}^{n}[\hat{\mathbf{a}}(\mathbf{x})\cdot\mathbf{S}^{\alpha}(\mathbf{x})]^2\right] . \tag{2.7}$$

We will now assume that local easy axes $\hat{\mathbf{a}}(\mathbf{x})$ are completely uncorrelated (although this should not be quite true in a real amorphous metal[22]), and then $P\{\hat{\mathbf{a}}\}$ can be factorized, i.e.,

$$P\{\hat{\mathbf{a}}(\mathbf{x})\}=\prod_{\mathbf{x}}p[\hat{\mathbf{a}}(\mathbf{x})] ,$$

$p[\hat{\mathbf{a}}(\mathbf{x})]$ being the probability distribution of unique ion

easy axes directions. Then integral in (2.7) can be factorized, obtaining

$$G\{\sigma(\mathbf{x})\}=\sum_{\mathbf{x}} g[\sigma(\mathbf{x})]$$

with the energy density given by

$$e^{-g(\sigma)}=\int d^m\hat{\mathbf{a}}\,p(\hat{\mathbf{a}})\exp\left[D_0\sum_{\alpha=1}^{n}(\hat{\mathbf{a}}\cdot\mathbf{S}^\alpha)^2\right]. \tag{2.8}$$

It can be shown[18] that the free energy per degree of freedom of the system described by H_{eff} is equal, in the limit $n\to 0$, to that of the original spin system.

We will now make the further assumption for an amorphous solid by considering a completely isotropic distribution of CEF easy axes,[18] i.e.,

$$p(\hat{\mathbf{a}})=\left[\int d^m\hat{\mathbf{a}}\right]^{-1}=\Gamma(m/2)/2\pi^{m/2}\,; \tag{2.9}$$

this assumption has been confirmed by Cochrane *et al.*[23] on the basis of a random packing of atomic spheres. Then Eq. (2.8) becomes

$$e^{-g(\sigma)}=\frac{1}{\int d^m\hat{\mathbf{a}}}\int d^m\hat{\mathbf{a}}\exp\left[D_0\sum_{i,j=1}^{m}\hat{\mathbf{x}}_i\hat{\mathbf{x}}_j\sum_{\alpha=1}^{n}S_i^\alpha S_j^\alpha\right]. \tag{2.10}$$

We now expand e^{-g} up to second order as well as the exponential within the integral and solve for the second-order equation in g finding[18,19]

$$g(\sigma)=-\frac{D_0}{m}|\sigma|^2+\frac{D_0^2}{m^2(m+2)}|\sigma|^4-\frac{D_0^2}{m(m+2)}\sum_{ij}\sum_{\alpha\beta}S_i^\alpha S_i^\beta S_j^\alpha S_j^\beta+O(|\sigma|^6)\,. \tag{2.11}$$

Finally, we obtain for the effective Hamiltonian,

$$H_{\text{eff}}=-J_0\sum_{\mathbf{x},\delta,\alpha}\mathbf{S}^\alpha(\mathbf{x})\cdot\mathbf{S}^\alpha(\mathbf{x}+\delta)-\frac{D_0}{m}\sum_{\mathbf{x},\alpha}\mathbf{S}^\alpha(\mathbf{x})\cdot\mathbf{S}^\alpha(\mathbf{x})+\beta\frac{D_0^2}{m^2(m+2)}\sum_{\alpha,\beta,\mathbf{x}}\sum_{i,j}S_i^\alpha(\mathbf{x})S_j^\beta(\mathbf{x})S_i^\alpha(\mathbf{x})S_j^\beta(\mathbf{x})$$
$$-\beta\frac{D_0^2}{m(m+2)}\sum_{\alpha,\beta,\mathbf{x}}\sum_{i,j}S_i^\alpha(\mathbf{x})S_i^\beta(\mathbf{x})S_j^\alpha(\mathbf{x})S_j^\beta(\mathbf{x})\,, \tag{2.12}$$

where we will assume that the exchange interaction is positive ($J_0>0$), in agreement with our findings for $R_{40}Y_{23}Cu_{37}$ amorphous alloys. The third term in (2.12) is clearly repulsive and reduces to $Nn^2|\mathbf{S}|^4$, and will be discarded, because it does not contribute to the order.[19] The second term merely produces a shift in the paramagnetic Curie temperature with an effective exchange interaction $J_0^*=J_0-D_0/m$. The main result of the Aharony model is that the fourth term has a form identical to the quartic spin term for a random exchange Ising spin system if one merely changes the *site* indices by spin *component* indices. Therefore, the RMA system can have a spin-glass transition if D_0 is sufficiently large.[19] This is in good agreement with the result previously mentioned that there cannot be long-range ferromagnetic order in a RMA system for $d<4$. Therefore, we will now follow the same kind of formalism as that for an Ising random exchange spin glass with short-range interactions (Edwards-Anderson spin glass[24]). We will perform the calculation for our general Heisenberg m-component spin.

$$F=-\frac{1}{\beta}\lim_{n\to 0}\frac{1}{n}\left[\mathrm{Tr}_n\exp\left[\beta J_0^*\sum_{(\mathbf{x},\delta,\alpha)}\mathbf{S}^\alpha(\mathbf{x})\cdot\mathbf{S}^\alpha(\mathbf{x}+\delta)+\beta^2\frac{D_0^2}{m(m+2)}\sum_{ij}\sum_{\alpha\beta}\sum_{\mathbf{x}}S_i^\alpha(\mathbf{x})S_j^\alpha(\mathbf{x})S_i^\beta(\mathbf{x})S_j^\beta(\mathbf{x})\right]-1\right]. \tag{2.13}$$

Terms with $\alpha=\beta$ and $\alpha\neq\beta$ must be treated separately,[25] and therefore we split the RMA term as

$$\sum_{ij}\sum_{\alpha\beta}S_i^\alpha S_j^\alpha S_i^\beta S_j^\beta=\sum_{ij}\sum_{\alpha}(S_i^\alpha)^2(S_j^\alpha)^2+2\sum_{ij}\sum_{(\alpha\beta)}S_i^\alpha S_i^\beta S_j^\alpha S_j^\beta\,, \tag{2.14}$$

where the first term in (2.14) has the form of a quadrupolar interaction, while the second is the one leading to the RMA spin-glass ordering.[26] In the spirit of the Sherrington-Kirkpatrick (SK) model[24,25] we perform a mean-field (MF) approximation by writing

$$\sum_{ij}\sum_{\alpha}(S_i^\alpha)^2(S_j^\alpha)^2\simeq m\sum_{i}\sum_{\alpha}(p_\alpha(S_i^\alpha)^2-p_\alpha^2/2)\,,$$
$$\sum_{ij}\sum_{(\alpha\beta)}S_i^\alpha S_i^\beta S_j^\alpha S_j^\beta\simeq m\sum_{i}\sum_{(\alpha\beta)}(q_{\alpha\beta}S_i^\alpha S_i^\beta-q_{\alpha\beta}^2/2)\,, \tag{2.15}$$

and defining MF parameters in the replicated system in the form

$$p_\alpha=\frac{1}{m}\sum_{j=1}^{m}\langle(S_j^\alpha)^2\rangle_n\,, \tag{2.16a}$$

$$q_{\alpha\beta}=\frac{1}{m}\sum_{j=1}^{m}\langle S_j^\alpha S_j^\beta\rangle_n\,, \tag{2.16b}$$

and where $\alpha\neq\beta$ in (2.16b).

We will now make the ansatz that all the p's and q's are the same at the extremal of F, i.e., $p_\alpha \equiv p$ and $q_{\alpha\beta} \equiv q$; then substituting (2.15) and (2.16) in (2.13) we readily obtain

$$F=\beta^{-1}\lim_{n\to 0}\frac{1}{n}\left[1-\mathrm{Tr}_n\exp\left\{\sum_{\alpha,\mathbf{x}}\left[\beta J_0^* zM\left[S_z^\alpha(\mathbf{x})-\frac{M}{2}\right]\right]+\beta^2\frac{D_0^2 m}{m(m+2)}\sum_{\alpha,\mathbf{x},i}[p(S_i^\alpha)^2-p^2/2]\right.\right.$$
$$\left.\left.+2\beta^2\frac{D_0^2 m}{m(m+2)}\sum_{(\alpha\beta)}\sum_{\mathbf{x}}\sum_i(qS_i^\alpha S_i^\beta-q^2/2)\right\}\right], \tag{2.17}$$

where we have made the further approximation of assuming only exchange among the axial spin components (this is strictly true when introducing the MF approximation with average induced magnetization, M, only along the field axis). Now, we follow the usual procedure of rearranging $\sum_i\sum_{(\alpha,\beta)}S_i^\alpha S_i^\beta$ in the form[24,25]

$$\sum_i\sum_{(\alpha\beta)}S_i^\alpha S_i^\beta=\frac{1}{2}\sum_i\left[\sum_\alpha S_i^\alpha\right]^2-\frac{1}{2}\sum_{i\alpha}(S_i^\alpha)^2, \tag{2.18}$$

making use of the Hubbard-Stratanovich identity

$$\exp\left[\frac{a^2}{2}\left[\sum_\alpha S^\alpha\right]^2\right]=\int_{-\infty}^{\infty}\exp\left[-\frac{x^2}{2}+ax\sum_\alpha S^\alpha\right]\frac{dx}{\sqrt{2\pi}}, \tag{2.19}$$

and using again the replica trick formula (2.4). We now assume an Ising approximation and make $S_i^\alpha=0$ for $i\neq z$. Then we obtain for the free energy

$$-\beta\frac{F}{N}=\beta^2\frac{\Delta^2}{4}(q^2-p^2)-\tfrac{1}{2}\beta J_0^* zM^2+\int_{-\infty}^{\infty}\frac{dx}{\sqrt{2\pi}}e^{-x^2/2}\ln\mathrm{Tr}\exp[\alpha S_z^2+(\gamma x+J_0^* zM+g\mu_\beta H)S_z], \tag{2.20}$$

and where

$$\Delta^2=\frac{2}{m+2}D_0^2,\quad \gamma=\beta\sqrt{q}\left[\frac{2}{m+2}\right]^{1/2}D_0,$$
$$\alpha=\frac{\beta^2 D_0^2}{m+2}(p-q). \tag{2.20'}$$

This result is identical to the one obtained for random exchange SG,[24,25,27] if we change

$$(\beta^2\tilde{J}^2)/2\to(\beta^2 D_0^2)/m(m+2)$$

and $z\to m$, i.e., the spin *components* play an equal role as the *site* indices (here $\tilde{J}$ is the standard deviation of the Gaussian random exchange distribution). Notice that an applied magnetic field term has been introduced in (2.20) (where g is the Landé factor and μ_B the Bohr magneton); this introduction is trivially resulting from the Zeeman extra-term $-g\mu_B\sum_{\mathbf{x}}\mathbf{S}^\alpha(\mathbf{x})\cdot\mathbf{H}$. The extremal of F against p, q, and M will give the equilibrium values of these parameters. From the equations

$$(\partial F/\partial q)=(\partial F/\partial p)=(\partial F/\partial M)=0,$$

one readily obtains,

$$p=\int_{-\infty}^{\infty}\frac{dx}{\sqrt{2\pi}}e^{-x^2/2}\langle S_z^2\rangle, \tag{2.21a}$$

$$q=p-\frac{1}{\gamma}\int_{-\infty}^{\infty}\frac{dx}{\sqrt{2\pi}}xe^{-x^2/2}\langle S_z\rangle, \tag{2.21b}$$

$$M=\int_{-\infty}^{\infty}\frac{dx}{\sqrt{2\pi}}e^{-x^2/2}\langle S_z\rangle, \tag{2.21c}$$

where

$$\langle A\rangle=\mathrm{Tr}\{A\exp[\alpha S_z^2+S_z(\gamma x+\beta zJ_0^* M+\beta g\mu_B H)]\}/\mathrm{Tr}\exp[\ldots],$$

is the thermal average of the operator A. Again expressions (2.21a)–(2.21c) are identical to the SK model[24,25,27] ones as they should be.

It will become useful later, in order to compare our model of magnetostriction with experiment, to obtain the expression for the spin-glass order temperature, T_{SG}, within the present model of RMA. Expression (2.21b) for q can be also written, for integer spin, in the form

$$q=\int_{-\infty}^{\infty}\frac{dx}{\sqrt{2\pi}}e^{-x^2/2}\left[\frac{\sum_{n=-S}^{+S}ne^{n^2\alpha}\sinh(n\gamma x)}{\sum_{n=-S}^{+S}e^{n^2\alpha}\cosh(n\gamma x)}\right], \tag{2.22}$$

where we have made $H=M=0$. Expanding now the hyperbolic functions for small $q(T\simeq T_{\mathrm{SG}})$, after some straightforward calculations we obtain

$$K_B T_{\mathrm{SG}}=\pm\left[\frac{2}{m+2}\right]^{1/2}D_0\left[\frac{\sum_{m_S}m_S^2\exp(m_S^2\alpha_{\mathrm{SG}})}{\sum_{m_S}\exp(m_S^2\alpha_{\mathrm{SG}})}\right], \tag{2.23}$$

with

$$\alpha_{SG}=(k_B T_{SG})^{-2}[D_0^2/(m+2)]p(T_{SG}) ,$$

and $m_S=(1,\ldots,+S)$. An expression completely similar is obtained for half-integer S (indeed, for a rare earth, S must be substituted by J, the total angular quantum number). Expression (2.23) is a generalization for high-spin values of the Chen and Lubensky[19] one, obtained using a continuous Ginzburg-Landau-Wilson approximation.

B. Magnetoelastic coupling in RMA spin glasses

1. *Anisotropy of axial character*

We will assume that the effect of the magnetoelastic coupling of the spin to the axial CEF gradient is to produce some rearrangement of the atomic environment of the R ion probe in order to modify the effective CEF strength of parameter D_0, but maintaining essentially constant the local easy axis direction $\hat{\mathbf{a}}(x)$. Although rearrangement of the local easy axes cannot be, in principle, ruled out, we will assume that the situation is likely the same as for crystalline materials, where it is assumed that the easy axis directions do not change due to the magnetostrictive distortions, the only source of magnetostriction being the dependence of the anisotropy energy with strain.[28] Now, if the CEF has to maintain the same axial symmetry as the unperturbed (2.1) one, the local strain that can couple to this CEF is $\epsilon_{\hat{a}\hat{a}}$, the strain *projected* along the local easy axis. Then the magnetoelastic coupling Hamiltonian will have the form

$$H_{ms}=-M_2\sum_{\mathbf{x}}[\hat{\mathbf{a}}(\mathbf{x})\cdot\mathbf{S}(\mathbf{x})]^2\epsilon_{\hat{a}\hat{a}}(\mathbf{x}) , \tag{2.24}$$

where according with the preceding discussion, $M_2=(\partial D_0/\partial\epsilon_{\hat{a}\hat{a}})$ is the magnetoelastic coupling parameter. This parameter is assumed to be homogeneous as for the unperturbed CEF parameter D_0, due to the reasons explained before. The strained system will get the equilibrium if an elastic energy of the form

$$H_{el}=\tfrac{1}{2}C_e\sum_{\mathbf{x}}[\epsilon_{\hat{a}\hat{a}}(\mathbf{x})]^2 , \tag{2.25}$$

is also present, and where C_e is some average elastic constant, assumed to be invariant across the solid.

Under the application of a polarizing magnetic field, $\mathbf{H}$, assumed uniform across the material, the solid will be magnetostrictively strained, and we will make the main assumption of assuming the strain to be along the field axis ($\hat{\mathbf{z}}$) and to be also uniform, i.e., ϵ_{zz}. In principle, local nonuniform strains are possible in an amorphous solid. However, this would be made at the expense of enormous amounts of elastic energy in the interfaces of regions of different strain directions (the appearance even of dislocations can be easily imagined). On the other hand, a uniform strain can couple to the local square magnetization induced by the field $[S_z(\mathbf{x})]^2$ as it will be shown. Moreover, a nonuniform strain will produce an elastic extra energy of $\mathbf{k}\neq 0$ phonon character, which is difficult to imagine in a purely static situation. Finally the *local* strain $\epsilon_{\hat{a}\hat{a}}$ coupling to the CEF produced by ϵ_{zz} will be

$$\epsilon_{\hat{a}\hat{a}}=\epsilon_{zz}\cos^2\theta(\mathbf{x}) , \tag{2.26}$$

where $\theta(\mathbf{x})$ is the angle formed by the local easy axis with the applied field axis ($\hat{\mathbf{z}}$).

We will now make full use of the previous replica technique in order to derive the effective Hamiltonian. This has the form

$$\tilde{H}_{ms}=-\sum_{\mathbf{x}}g(\mathbf{x},\boldsymbol{\sigma}) , \tag{2.27}$$

where the energy density is given by

$$e^{-g(\mathbf{x},\sigma)}=\frac{1}{\int d^m\hat{\mathbf{a}}}\int d^m\hat{\mathbf{a}}\exp\left[(D_0+M_2\epsilon_{\hat{a}\hat{a}})\sum_{\alpha=1}^{n}(\hat{\mathbf{a}}\cdot\mathbf{S}^\alpha)^2\right] . \tag{2.28}$$

Expansion of the exponentials up to second order and resolution of the second-order equation in $g(\boldsymbol{\sigma})$ produces the following magnetoelastic energy density:

$$\begin{aligned}g_{ms}(\boldsymbol{\sigma})=&-M_2\epsilon_{zz}\sum_{i,j}\langle\hat{\mathbf{x}}_i\hat{\mathbf{x}}_j\hat{\mathbf{x}}_1^2\rangle\sum_{\alpha=1}^{n}S_i^\alpha S_j^\alpha-D_0M_2\epsilon_{zz}\left\langle\left[\sum_{ij}\hat{\mathbf{x}}_i\hat{\mathbf{x}}_j\hat{\mathbf{x}}_1\sum_\alpha S_i^\alpha S_j^\alpha\right]^2\right\rangle\\&-\tfrac{1}{2}M_2^2\epsilon_{zz}^2\left\langle\left[\sum_{ij}\hat{\mathbf{x}}_i\hat{\mathbf{x}}_j\hat{\mathbf{x}}_1^2\sum_\alpha S_i^\alpha S_j^\alpha\right]^2\right\rangle+\tfrac{1}{2}C_e\epsilon_{zz}^2\langle x_1^4\rangle ,\end{aligned} \tag{2.29}$$

where the first two terms are magnetoelastic coupling ones, the third is a "morphic" term affecting the elastic constants values, and the last term is the elastic energy one. $\hat{\mathbf{x}}_i$ are the direction cosines of the local easy axis. We will neglect the morphic term; the term with coefficient D_0M_2 is a perturbation of the term responsible for the spin-glass order. We obtain the following types of average angular integrals:

$$\begin{aligned}\langle\hat{\mathbf{x}}_i\hat{\mathbf{x}}_j\hat{\mathbf{x}}_k\hat{\mathbf{x}}_l\rangle&=\frac{1}{m(m+2)}(\delta_{ij}\delta_{kl}+\delta_{ik}\delta_{jl}+\delta_{il}\delta_{jk}) ,\\\langle\hat{\mathbf{x}}_i^2\hat{\mathbf{x}}_j^2\hat{\mathbf{x}}_k^2\rangle&=\frac{1}{m(m+2)(m+4)}\quad(i\neq j\neq k) ,\\\langle\hat{\mathbf{x}}_i^3\hat{\mathbf{x}}_j\hat{\mathbf{x}}_k\hat{\mathbf{x}}_l\rangle&=\frac{1}{m(m+2)(m+4)}[3(\delta_{ij}\delta_{kl}+\delta_{ik}\delta_{jl}+\delta_{il}\delta_{jk})+6\delta_{ij}\delta_{ik}\delta_{il}] ,\end{aligned} \tag{2.30}$$

where $\langle \cdots \rangle$ are averages over the isotropic distribution $p(\hat{\mathbf{a}})$ of random CEF local anisotropy axes, i.e.,

$$\langle(\cdots)\rangle = \frac{1}{\int d^m\hat{\mathbf{a}} p(\hat{\mathbf{a}})} \int d^m\hat{\mathbf{a}}(\cdots)p(\hat{\mathbf{a}}) . \tag{2.31}$$

The magnetoelastic term in M_2 then becomes

$$\frac{-M_2\epsilon_{zz}}{m(m+2)} \sum_{\alpha=1}^{n} [3(S_z^\alpha)^2+(S_x^\alpha)^2+(S_y^\alpha)^2] , \tag{2.32}$$

and for $\mathbf{H}$ applied along $\hat{\mathbf{z}}$ we will neglect terms in $[S_x]^2$ and $[S_y]^2$, i.e., we restrict to an Ising approximation. Notice that in the plane normal to $\hat{\mathbf{z}}\|\mathbf{H}$ the magnetoelastic coupling Hamiltonian has cylindrical symmetry as it should be.

The other magnetoelastic term, after some rearrangements, becomes

$$-\frac{2D_0M_2}{m(m+2)(m+4)}\epsilon_{zz} \sum_{\alpha\beta}\sum_{ij} S_i^\alpha S_j^\alpha S_i^\beta S_j^\beta . \tag{2.33}$$

Collecting terms (2.32) and (2.33) we obtain the following magnetoelastic coupling plus elastic Hamiltonians:

$$\tilde{H}_{ms} = -\frac{3M_2}{m(m+2)}\epsilon_{zz} \sum_{\mathbf{x}}\sum_{\alpha} [S_z^\alpha(\mathbf{x})]^2 - \frac{2D_0M_2}{m(m+2)(m+4)}\epsilon_{zz} \sum_{\mathbf{x}}\sum_{\alpha\beta}\sum_{ij} S_i^\alpha(\mathbf{x})S_j^\alpha(\mathbf{x})S_i^\beta(\mathbf{x})S_j^\beta(\mathbf{x})$$
$$+\frac{1}{2}N\frac{3}{m(m+2)}C_e\epsilon_{zz}^2 . \tag{2.34}$$

According to this result the magnetostrictive distortion produces two effects: a main one of introducing an axial CEF anisotropy along the applied field direction, and an interaction identical to the one responsible for the SG order. This additional axial anisotropy clearly is macroscopic or coherent.

2. *Planar local anisotropy*

When locally, at site i, we have an easy plane $(\hat{\mathbf{x}}_i,\hat{\mathbf{y}}_i)$, i.e., $D_0<0$, in Eq. (2.31), the magnetoelastic coupling Hamiltonian for spherical symmetry must have the form

$$\tilde{H}^{\perp}_{ms} = -M_2^{\perp}(S_{x_i}^2+S_{y_i}^2)\epsilon_i^{\perp} , \tag{2.35}$$

where

$$\epsilon_i^{\perp} = (1/2)(\epsilon_{x_ix_i}+\epsilon_{y_iy_i})$$

is the irreducible strain for basal plane cylindrical symmetry. As before we now project the uniform macroscopic strain ϵ_{zz} along the basal plane in order to couple with the basal CEF, i.e.,

$$\epsilon_{x_ix_i} = \epsilon_{zz}\cos^2\theta ,$$

$$\epsilon_{y_iy_i} = \epsilon_{zz}\cos^2\gamma ,$$

where θ and γ are the angles between the local CEF axes $(\hat{\mathbf{x}}_i,\hat{\mathbf{y}}_i)$ with $\hat{\mathbf{z}}$. A calculation similar to the one done for local axial symmetry produces, within the Ising approximation, the effective axial coherent magnetoelastic anisotropy

$$\tilde{H}^{\perp}_{ms}+\tilde{H}_{el} = -M_2^{\perp}\epsilon_{zz}\frac{1}{m+2}\left[2-\frac{4}{m}\right]\sum_{\mathbf{x}}\sum_{\alpha}[S_z^\alpha(\mathbf{x})]^2+\tfrac{1}{2}C_e\frac{N}{m+2}\epsilon_{zz}^2 , \tag{2.36}$$

where terms in $(S_x^\alpha)^2$ and $(S_y^\alpha)^2$ have been neglected for induced magnetization along the $\hat{\mathbf{z}}$ axis, i.e., we adopt an Ising approximation.

C. Free energy and equilibrium strains

Following the same procedure outlined in Sec. II A, we obtain for the free energy including ferromagnetic exchange, RMA anisotropy and magnetoelastic coupling

$$\beta F = -N\left[\frac{\beta^2}{4}\Delta^{*2}(q^2-p^2)-\beta\frac{J_0}{2}zM^2+\int_{-\infty}^{\infty}\frac{dx}{\sqrt{2\pi}}e^{-x^2/2}\ln \mathrm{Tr}\exp[\alpha^*S_z^2+(\gamma^*x+\beta zJ_0M+\beta g\mu_B H)S_z]\right.$$
$$\left.-\frac{1}{2}\frac{3\beta C_e}{m(m+2)}\epsilon_{zz}^2\right] , \tag{2.37}$$

and where the ingredient parameters are modified by the magnetostrictive distortion in the form

$$(\Delta^*)^2=\frac{2}{m+2}D_{ef}^2 ,$$
$$\alpha^*=\beta^2\frac{D_{ef}^2}{m+2}(p-q)+\frac{3\beta M_2}{m(m+2)}\epsilon_{zz} , \tag{2.38}$$
$$\gamma^*=\beta\sqrt{q}\left[\frac{2}{m+2}\right]^{1/2}D_{ef} ,$$

with

$$D_{ef}^2=D_0^2\left[1+\frac{2}{m+4}\frac{M_2}{D_0}\epsilon_{zz}\right] , \tag{2.39}$$

being an effective CEF strength parameter.

The extremal of F against q, p, and M will give, as in Sec. II A, the equilibrium values for these parameters, which keep the same form as expressed by Eqs. (2.21a)–(2.21c), but instead now including the parameters given by Eqs. (2.38) and (2.39). The equilibrium magnetostrictive strain results from the condition $\partial F/\partial\epsilon_{zz}=0$ and from (2.37) it becomes

$$\epsilon_{zz}=\frac{M_2}{C_e}\left[p+\frac{1}{(m+4)}\frac{D_0}{K_BT}(p^2-q^2)\right] . \tag{2.40}$$

As can be seen, the magnetostrictive strain has two contributions: one is the quadrupolar contribution due to the CEF distortion, and the other is proportional to the thermodynamic internal energy, appearing also in the specific heat expression.[29,30] This term decreases rapidly with temperature and it will be generally neglected so on. It is useful to speculate about the extremal character of ϵ_{zz} as obtained from the condition $\partial F/\partial\epsilon_{zz}=0$. A quite straightforward calculation shows that

$$\frac{\partial^2F}{\partial\epsilon_{zz}^2}=\beta\frac{C_e}{m+2}+\int_{-\infty}^{\infty}\frac{dx}{\sqrt{2\pi}}e^{-x^2/2}\left[\left\langle\left[\frac{\partial}{\partial\epsilon_{zz}}(\alpha^*S_z^2+x\gamma^*S_z)\right]^2\right\rangle-\left\langle\frac{\partial}{\partial\epsilon_{zz}}(\alpha^*S_z^2+x\gamma^*S_z)\right\rangle^2\right] , \tag{2.41}$$

which is always a positive quantity, and therefore ϵ_{zz} given by Eq. (2.40) actually corresponds to a minimum of the magnetoelastic free energy.

Now the anisotropic magnetostriction producing a "tetragonal" distortion of the unperturbed spherical symmetry of the amorphous system is

$$\lambda_t=\tfrac{1}{2}(3\epsilon_{zz}-\omega) , \tag{2.42}$$

and from (2.40) it must be given by

$$\lambda_t=\frac{M_2}{2C_e}[3p-S(S+1)]=\frac{M_2}{C_e}\int_{-\infty}^{\infty}\frac{dx}{\sqrt{2\pi}}e^{-x^2/2}\langle\tilde{O}_2^0\rangle , \tag{2.43}$$

where

$$\tilde{O}_2^0=(1/2)[3S_z^2-S(S+1)]$$

is the quadrupolar Stevens operator. λ_t has the usual form of a magnetostrictive strain of CEF origin. In expression (2.43) besides the canonical thermal average, one has the average over the RMA disorder through the Gaussian distribution. Notice again that for R ions the spin **S** has to be substituted by the total angular momentum **J** through all the equations (2.21a)–(2.21c) and (2.43), and in this form they will be used from therein.

The expression for λ_t when the local anisotropy is planar is obtained in a similar way from the coherent anisotropy effective magnetoelastic Hamiltonian given by Eq. (2.36). One then obtains the same expression (2.43) by changing M_2/C_e by $(M_2^{\perp}/C_e)(2-4/m)$ [we again neglect a second-order term similar to the one in Eq. (2.40)].

III. EXPERIMENT: MAGNETOSTRICTION IN $R_{40}Y_{23}Cu_{37}$ AMORPHOUS ALLOYS

The samples of $R_{40}Y_{23}Cu_{37}$ (R =Tb, Dy, Ho, and Er) were prepared using the argon arc technique starting from the constituents: rare earths of 99.9% and Cu of 99.999% purities. Amorphous ribbons were prepared using the rotating wheel technique, the ribbons having an average width of 2 mm and ≈40 microns in thickness. The amorphous structure was checked using x-ray K_α copper radiation, broad maxima due to nearest neighbors ($2\theta\approx33°$) and next nearest neighbors ($2\theta\approx57°$) being observed. Small peaks of residual crystallinity were superficial inasmuch as they were removed by rubbing the ribbon surface with fine emery paper. The composition was checked as well using scanning electron microscopy and the energy dispersive x-ray microanalysis (EDAX) technique.

The magnetostriction measurements were performed using the well-known strain gauge technique,[31] using a

dummy gauge in order to compensate for thermal expansion and magnetoresistance in the gauges. The magnetic field was produced with a superconducting coil (up to 7 T) for the samples with Tb, Dy, and Er, and with a pulse field coil (up to 15 T) for the Ho alloy. In order to prevent the stiffness of the gauge, around 12 ribbons were glued together with *M*-600 bond agent (Micromeasurements, USA), forming a sort of composite, and the gauge (SK-350 Micromeasurements) was attached to it. The strain was measured using a sensitive dc bridge (for the continuous fields) and a 25 KHz modulation bridge (for the pulsed fields). Details of those apparatus are given, respectively, in Refs. 32 and 33. Magnetostriction was measured parallel ($\lambda_{\parallel}$) and perpendicular ($\lambda_{\perp}$) to the applied field in order to extract the volume strain, $\omega=\lambda_{\parallel}+2\lambda_{\perp}$, and the anisotropic one,

$$\lambda_t=\lambda_{\parallel}-\lambda_{\perp}[=(3/2)(\lambda_{\parallel}-\omega/3)] .$$

(Notice that, indeed, the strictions $\lambda_{\parallel}\equiv\epsilon_{zz}$ and $\lambda_{\perp}\equiv\epsilon_{xx}\equiv\epsilon_{yy}$, but we prefer to use the notation customarily used in magnetoelastic work.[31]) We present in Figs. 1–4 isotherms of parallel and perpendicular magnetostriction between about 4.2 and 150 K for the studied

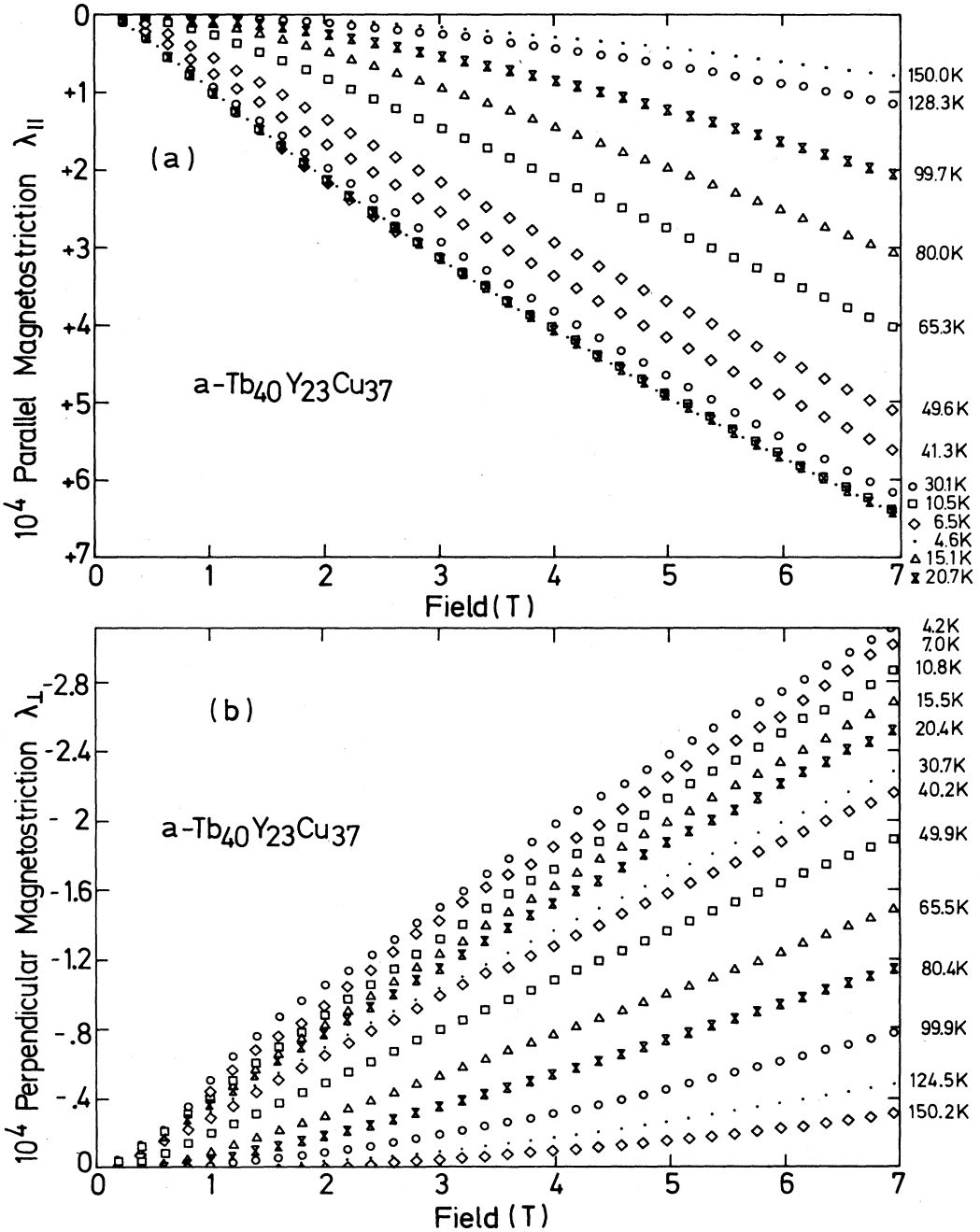

FIG. 1. Parallel, $\lambda_{\parallel}$, (a), and perpendicular, $\lambda_{\perp}$, (b), magnetostriction vs applied magnetic field isotherms for amorphous $Tb_{40}Y_{23}Cu_{37}$ alloy.

compounds. As it can be observed, magnetostriction changes almost linearly with field even well above T_{SG}, with no sign of saturation, the magnetostriction being a forced one. Magnetostriction is very large and remains so even well above T_{SG}. In Figs. 5(a)–5(d) we present the thermal variation of $\lambda_{\parallel}$ and $\lambda_{\perp}$ at the maximum applied field $H \simeq 7$ T; as it can be observed, $\lambda_{\perp} \approx -\lambda_{\parallel}/2$, and therefore ω is small in those materials. This means that the tetragonal distortion, ϵ_1^{γ}, of the spherical environment of a rare-earth probe ion is almost exclusively contributed by the axial distortion along the field axis z, i.e.,

$$\epsilon_1^{\gamma} = (3/\sqrt{6})(\epsilon_{zz} - \omega/3) \simeq (3/\sqrt{6})\epsilon_{zz} \ .$$

The only exception was the sample of Ho, where all the attempts to determine a measurable $\lambda_{\perp}$ were unsuccessful, the estimated $\lambda_{\perp} \approx 0$ at all temperatures. However, $\omega/3$ is as small as in the other compounds and therefore was neglected.

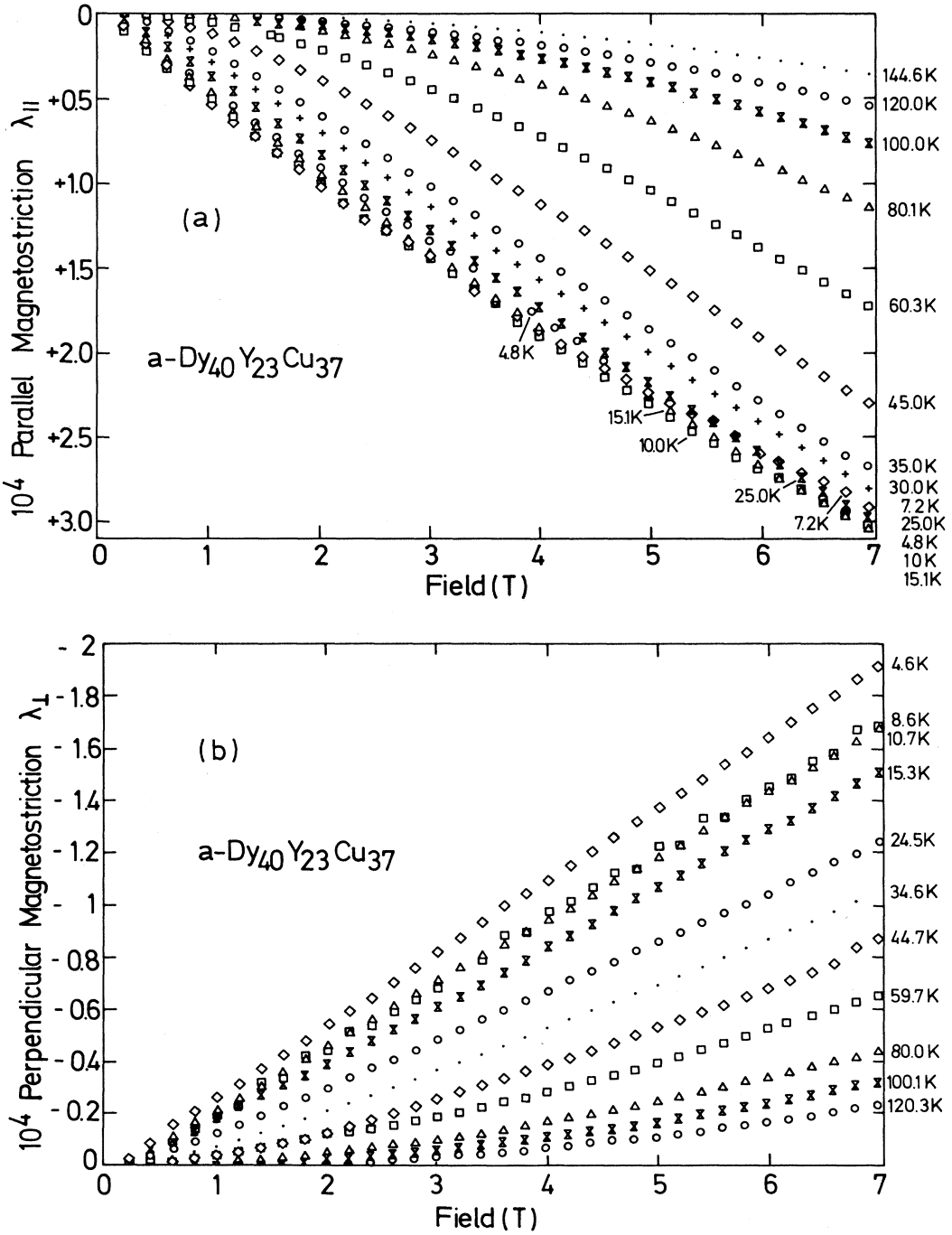

FIG. 2. Same as Figs. 1(a) and 1(b) for amorphous $Dy_{40}Y_{23}Cu_{37}$ alloy.

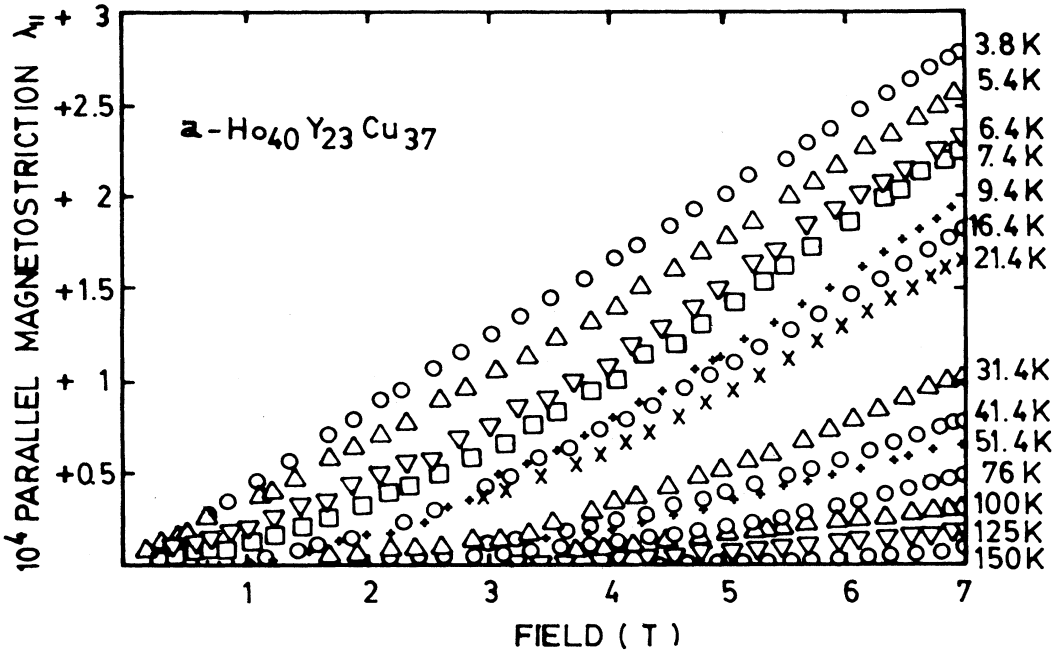

FIG. 3. Same as Figs. 1(a) and 1(b) for amorphous $Ho_{40}Y_{23}Cu_{37}$ alloy.

IV. RESULTS AND DISCUSSION

A. Comparison of model with magnetostriction experiment

We now proceed to quantitatively compare our theoretical model of magnetoelastic coupling in RMA spin glasses with the magnetostriction measurements quoted in Sec. III. To be more specific, we proceed to fit the thermal variation of the anisotropic magnetostriction, λ_t, at the maximum applied field $H \simeq 7$ T, using the model expression (2.43) derived in our theoretical model (Secs. II B 1, II B 2, and II C) [we neglect the second order contribution in (2.40) for the time being]. The two kinds of ions studied, Tb^{3+}, Dy^{3+}, and Ho^{3+} (Stevens coefficient $\alpha_J < 0$) and $Er^{3+}(\alpha_J > 0)$ allow us to test our model for locally uniaxial and planar anisotropies. To perform the fit we need to know the thermal variation of the spin-glass order parameter q and of the field-induced magnetization M. We have then proceeded to a self-consistent solution of Eqs. (2.21a), (2.21b), and (2.21c), for q, p, and M, respectively. In doing this we have two disposable parameters, the effective exchange parameter J_0^* and the CEF strength D_0. In Fig. 6 we show the thermal variations of q for the different compounds, as obtained from initial susceptibility measurements[17] (Sec. I) together with the theoretical calculation. J_0^* was obtained from the paramagnetic Curie temperature, $\Theta = zJ_0^*$, the values of Θ, obtained from the ac susceptibility, being shown in Table I. D_0 was initially fixed by setting q equal to zero at T_{SG} in Eq. (2.23). In Fig. 7 we show the thermal variation of the magnetization[11] at 7 T, together with the theoretical calculation. Theory predicts for Tb, Dy, and Ho compounds, low-temperature broad cusps, which are not observed at the large field of measurement, although the degree of agreement between theory and experiment is satisfactorily correct.

We show in Figs. 8(a)–8(d) the thermal variation of λ_t for the studied compounds, together with the theoretical calculation. The agreement with experiment is remarkably good. The values of D_0 used for the fit are shown in Table I. They were obtained from Eq. (2.23) solved in a self-consistent way. We have obtained that $D_0 > 0$ for the ions Tb^{3+}, Dy^{3+}, and Ho^{3+} for which $\alpha_J < 0$, which means that we have locally *uniaxial* anisotropy. In the case of Er^{3+}, with $\alpha_J > 0$, the parameter D_0 had to be taken negative (see Table I) in order to compute a reasonable thermal variation of λ_t. This means that we are in the presence of locally *planar* anisotropy, in agreement with $\alpha_J > 0$. However, the agreement is now (Er^{3+} ion) only qualitative. The calculated second-order contribution in Eq. (2.40) does not improve the fit substantially [see Fig. 8(d)], and one wonders whether fourth-order terms in the CEF magnetoelastic Hamiltonian would be responsible for such a discrepancy in the case of the Er^{3+} compound.

B. Comparison with CEF point charge model

It is always a useful practice to evaluate the magnetoelastic coupling parameters within the point-charge model (PCM). For an amorphous alloy, any irreducible distortion supported by spherical symmetry is suitable to calculate M_2, and we will choose the zero volume tetragonal mode, i.e.,

$$\epsilon_{zz} = \epsilon, \epsilon_{xx} = \epsilon_{yy} = -\epsilon/2 \ .$$

In a rare-earth amorphous alloy the random CEF poten-

tial felt by the rare-earth probe ion can be expanded in tesseral harmonics Z_{no}, and the second-order or axial term has the form[34]

$$V_{20}(R_j,\theta_j,\phi_j)=-\frac{4\pi}{5}|e|^2\alpha_J\langle r_{4f}^2\rangle\sum_j\frac{Z_j}{R_j^3}Z_{20}(\theta_j,\phi_j)\ , \tag{4.1}$$

where R_j are the distances of the ligand ions j (with charge Z_j) to the probe one, and (θ_j,φ_j) the polar angles referred to the local frame. α_J is the Stevens reduced matrix element and $\langle r_{4f}^2\rangle$ the average radial second moment for the $4f$ electrons.[35] We now express V_{20} in terms of cartesian ion coordinates, and distort the positions of the ligand ions within the mode mentioned, expanding V_{20} in powers of ϵ_1^γ, in order to obtain M_2.[36] If we furthermore perform the spatial average $[\langle\cdots\rangle_r$ in expression (4.2)] of the potential we finally obtain

$$M_2=\frac{\sqrt{6}}{4}|e|^2\alpha_J\langle r_{4f}^2\rangle\langle f(R_j,\theta_j)\rangle_r\ , \tag{4.2}$$

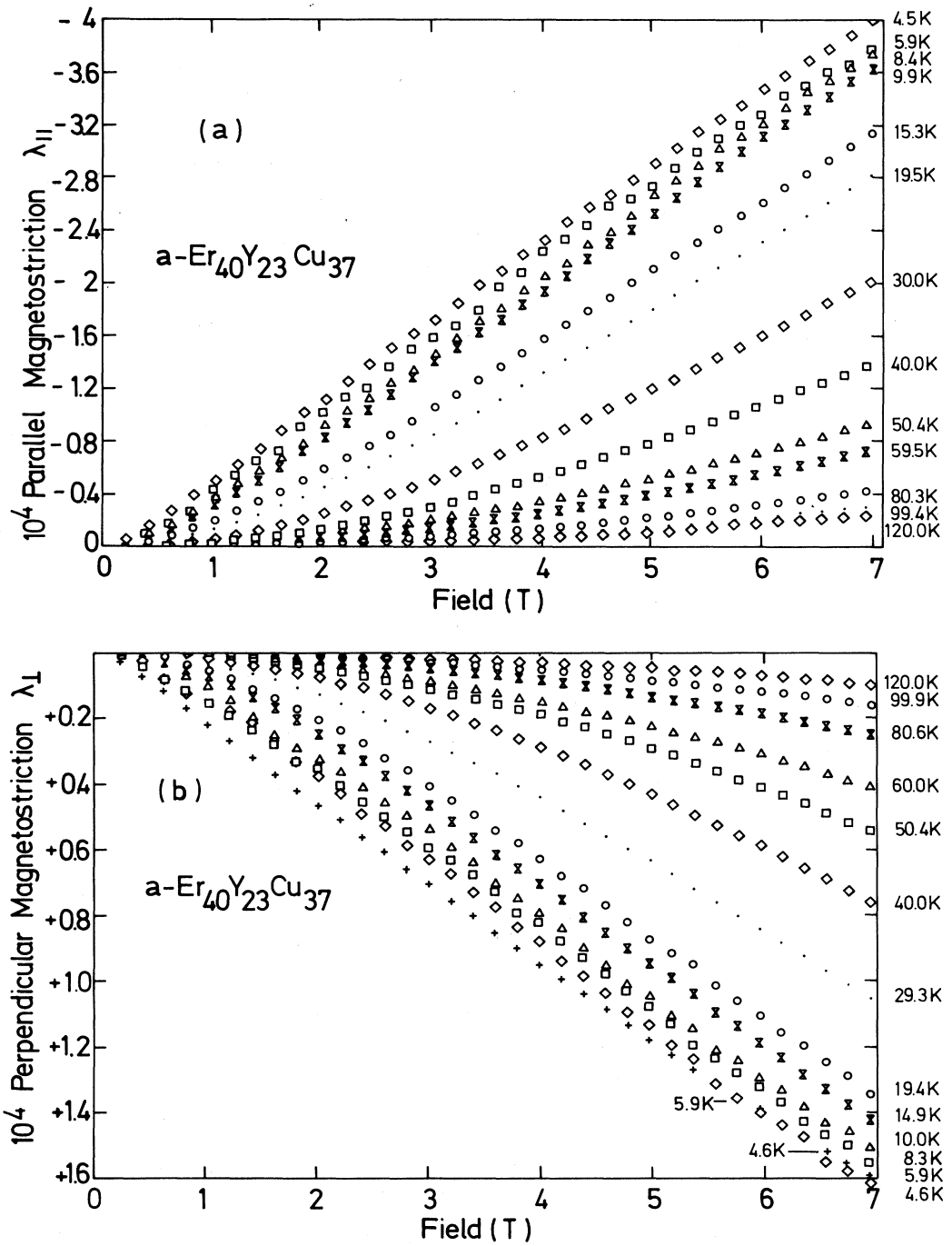

FIG. 4. Same as Figs. 1(a) and 1(b) for amorphous $Er_{40}Y_{23}Cu_{37}$ alloy.

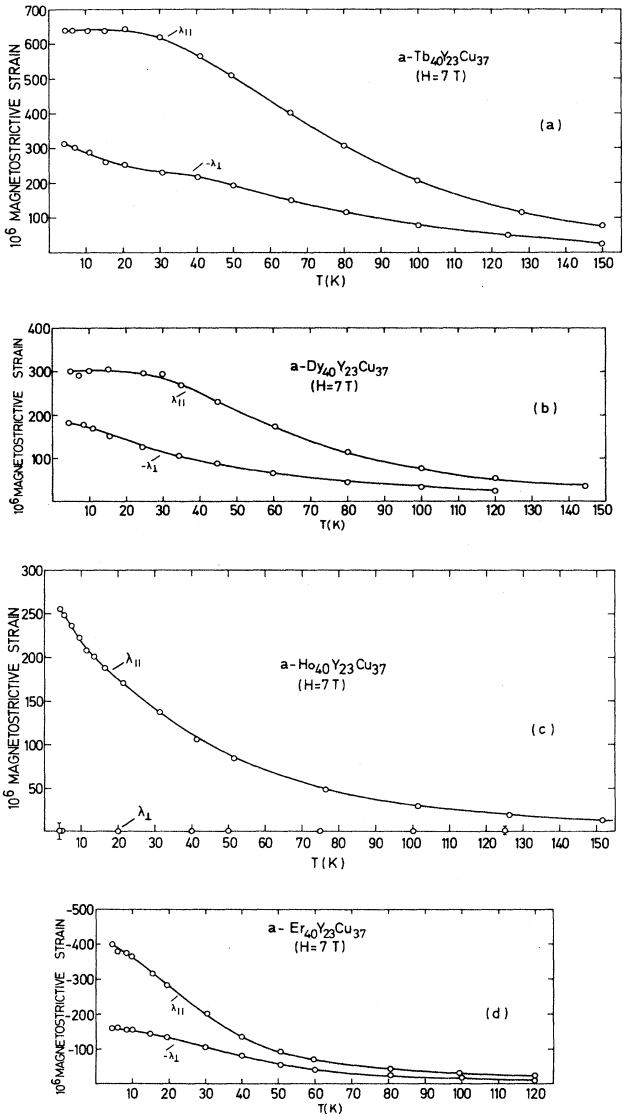

FIG. 5. (a) Thermal variation of measured parallel ($\lambda_{\parallel}$) and perpendicular ($\lambda_{\perp}$) magnetostriction at the maximum applied magnetic field of 7 T, for the a-$Tb_{40}Y_{23}Cu_{37}$ alloy (the continuous lines are guides for the eye). (b) Same as Fig. 5(a) for a-$Dy_{40}Y_{23}Cu_{37}$ alloy. (c) Same as Fig. 5(a) for a-$Ho_{40}Y_{23}Cu_{37}$ alloy. (d) Same as Fig. 5(a) for a-$Er_{40}Y_{23}Cu_{37}$ alloy.

where

$$f(R_j,\theta_j)=\sum_j (Z_j/R_j^3)[(\tfrac{15}{2})\cos^4\theta_j-6\cos^2\theta_j+\tfrac{1}{2}] .$$

This result is similar to the one earlier obtained by Suzuki and Egami,[37] and for a perfectly spherical or isotropic angular distribution of ions, M_2 becomes zero. These authors suggested that magnetostriction will become non-null if one introduces some sort of screening or antiscreening by the conduction electrons within the PCM. We also believe that a very slight deviation from perfect local spherical symmetry is able to explain a non-null magnetostriction in amorphous rare-earth alloys giving non-null average values for $f(R_j,\theta_j)$. In fact, if we as-

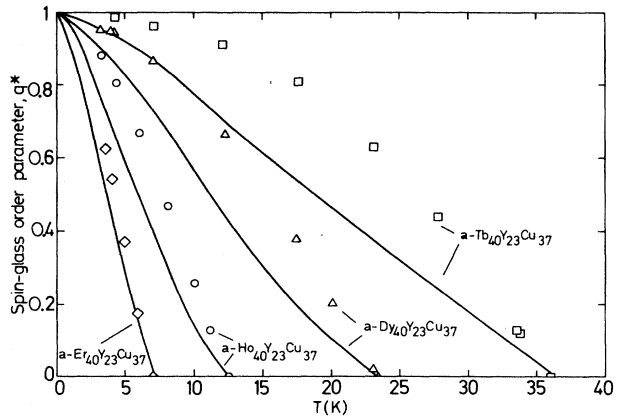

FIG. 6. Thermal variation of the RMA zero-field spin glass order parameter q^* (normalized for a rare-earth ion as $q^*=q/J^2$) for the amorphous alloys $R_{40}Y_{23}Cu_{37}$ [$R=$(□) Tb; (△) Dy; (○) Ho; and (◇) Er]. The continuous lines are the theoretical calculations according to model Eqs. (2.21b) and (2.22) (see Sec. II for details).

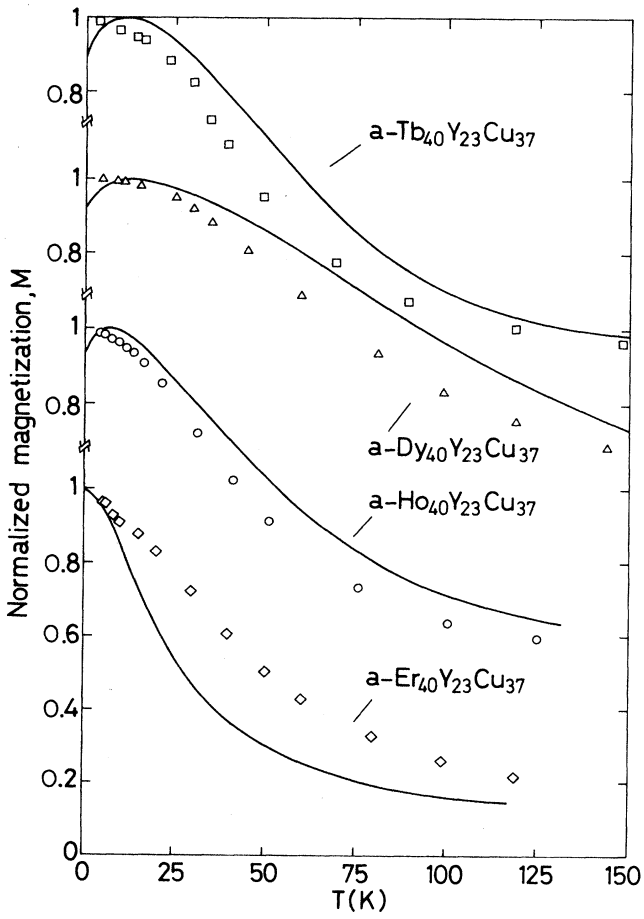

FIG. 7. Thermal variation of the induced magnetization, M, by an applied magnetic field $H=7$ T for the a-$R_{40}Y_{23}Cu_{37}$ alloys [(□) Tb; (△) Dy; (○) Ho; and (◇) Er]. The values of $M(T,H)$ have been normalized by the extrapolated one $M(0\text{ K}; 7\text{ T})$. The continuous lines are the theoretical calculations according to model Eq. (2.21c) (see Sec. II for details).

sume that $\alpha \leq \theta_j \leq \pi - \alpha$, with α near but not exactly equal to zero, and we calculate $\langle f(R_j,\theta_j)\rangle_r$ averaging over an isotropic distribution of local easy axes, we obtain

$$M_2 = \frac{\sqrt{6}}{4}|e|^2 \alpha_J \langle r_{4f}^2 \rangle \left\langle \sum_j \frac{Z_j}{R_j^3} \right\rangle_r \left(\tfrac{3}{2}\cos^4\alpha - 2\cos^2\alpha + \tfrac{1}{2}\right) . \tag{4.3}$$

In any case, assuming equal atomic environment for the whole series of compounds, the values of M_2 are controlled by $\alpha_J \langle r_{4f}^2 \rangle$. According to Table I, the experimentally determined relative values of M_2 ($M_2^{\perp}$ for $Er_{40}Y_{23}Cu_{37}$) are, respectively, for the Tb, Dy, Ho, and Er compounds, $+1{:}+0.31{:}+0.18{:}-0.28$, in remarkably good agreement with the prediction of our PCM Eq. (4.2), which is $+1{:}+0.32{:}+0.20{:}-0.25$. Therefore, the PCM (either with electron screening or distortion of perfect spherical local symmetry) is remarkably well accomplished in the present amorphous alloys.

It is now worthwhile to estimate the deviations from perfect sphericity in order to explain with formula (4.3) the values obtained for the magnetoelastic coupling parameters M_2. In order to evaluate the spatial average in Eq. (4.3) we should know the radial distribution functions $g_{ij}(r)$ for the different pairs of ions. We will make the assumption of assigning zero charge to the Cu atoms and take $Z_j = +3$ for the rare-earth ions. According to Hunter[38] measurements, $g(r)$ for the isomorphous alloy $Y_{63}Cu_{37}$ gives an average distance $\langle R_{Y-Y} \rangle = 3.58$ Å and a number of NN of ≈ 6. In this way we estimate that

$$\left\langle \sum_j (Z_j/R_j^3) \right\rangle_r \approx 3.9 \times 10^{23} \text{ cm}^{-3} .$$

Then, from Eq. (4.3), and using the experimental values of M_2 of Table I, we obtain that the values of α vary between 50° and 52° for the present series of compounds, showing only a slight, although significant, distortion

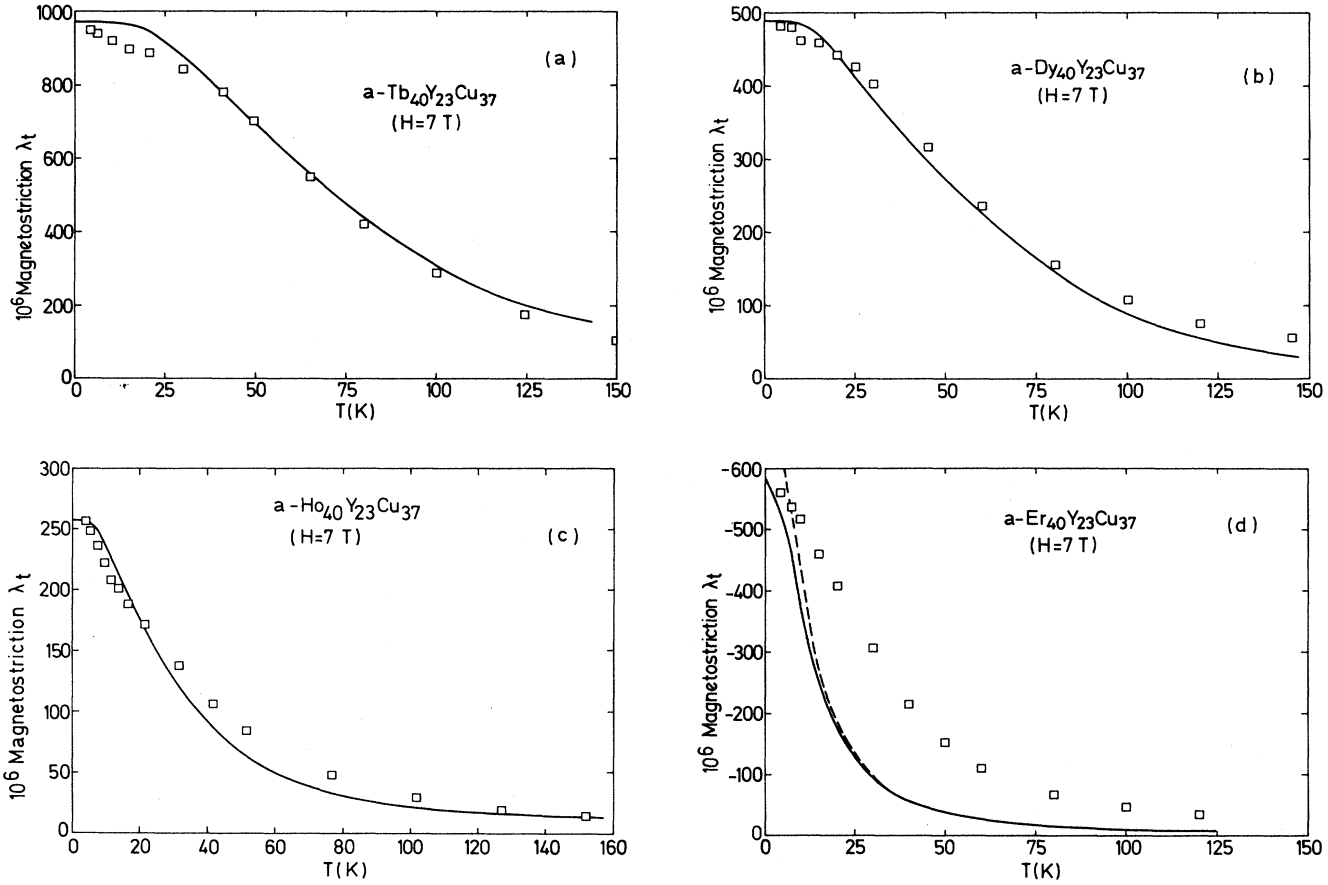

FIG. 8. (a) Thermal variation of the anisotropic magnetostriction, λ_t, at an applied magnetic field $H = 7$ T for the amorphous alloy $Tb_{40}Y_{23}Cu_{37}$. The continuous line is the theoretical calculation according to model Eq. (2.43) (see Sec. II for details). The model parameters [see Eqs. (2.1), (2.6), (2.24), and (2.25) for definitions] resulting from the fit are: $\Theta = 7.5$ K, $D_0 = 3$ K, and $M_2/C_e = +29.2 \times 10^{-6}$ (see also Table I). (b) Same as Fig. 8(a) for the *a*-$Dy_{40}Y_{23}Cu_{37}$ alloy, with fitting parameters $\Theta = 4$ K, $D_0 = 1.25$ K, and $M_2/C_e = +9.2 \times 10^{-6}$. (c) Same as Fig. 8(a) for the *a*-$Ho_{40}Y_{23}Cu_{37}$ alloy, with fitting parameters $\Theta = 1.3$ K, $D_0 = 0.6$ K, and $M_2/C_e = +4.4 \times 10^{-6}$. (d) Same as Fig. 8(a) for the *a*-$Er_{40}Y_{23}Cu_{37}$ alloy, with fitting parameters $\Theta \approx 0$ K, $D_0 = -0.37$ K, and $M_2^{\perp}/C_e = -8.3 \times 10^{-6}$ [$M_2^{\perp}$ is the planar local CEF symmetry magnetoelastic coupling parameter, see (2.36)]. The continuous line is the theoretical calculation according to model Eq. (2.43), and the broken one also includes the computed second-order term in (2.40).

from perfect sphericity. The structure factor $F(\alpha)$ in (4.3) varies between $\cong -0.038$ and $\cong -0.065$, i.e., is very small [instead, for a crystalline alloy, $F(\alpha)$ usually is quite large].

V. CONCLUSIONS

Several main conclusions can be extracted from this research. A theoretical model has been proposed to explain magnetostriction in random magnetic anisotropy (RMA) spin glasses, with positive exchange interaction. The model assumes a *homogeneous* strain along the applied field axis (which, in turn, is locally projected along the local crystal-field axis) and uses the standard replica method. The assumed single-ion magnetoelastic crystal-field coupling [see Eq. (2.24)] induces an additional coherent macroscopic anisotropy along the applied magnetic field axis (plus a term of identical nature of the one responsible for the spin-glass behavior). The model works either for axial or planar local anisotropies. The main conclusion of our model is that the bulk anisotropic striction becomes proportional to the average (thermal and over the disorder) quadrupolar moment.

The proposed model fits quantitatively and remarkably well the thermal variation of the anisotropic magnetostriction, λ_t, for the RMA amorphous magnets $R_{40}Y_{23}Cu_{37}$ (with R = Tb, Dy, Ho, and Er). λ_t is quite large for those systems and remains so well above the spin-glass temperature. A result of the fit above is the determination of the effective ferromagnetic exchange coupling parameter, J_0^*, of the random crystal-field strength, D_0, and of the magnetoelastic coupling parameter, M_2, for the present series of compounds. The signs and strengths of the experimental values of D_0 and M_2 (see Table I) agree remarkably well with the developed single-ion point-charge model for those amorphous magnets. It is also suggested that the existence of finite magnetostriction in amorphous magnets is related to the existence of a slight distortion of the otherwise perfectly spherical local symmetry. In this sense magnetostriction perhaps manifests itself as a unique technique to show up deviations from perfect local spherical atomic distribution in amorphous magnetic materials.

ACKNOWLEDGMENTS

We are indebted to Professor E. W. Lee, Professor B. D. Rainford, and Dr. C. Cornelius for the experimental facilities at the University of Southampton, and to Dr. K. A. Mohammed for assistance with the preparation of the amorphous ribbons. Assistance of Dr. P. A. Algarabel with the pulsed magnetic field measurements and Dr. C. Rillo with some high-field magnetization measurements are acknowledged. We also warmly acknowledge very useful suggestions and discussions with Professor M. B. Salamon, Professor E. Fradkin, and Dr. P. Goldbart (University of Illinois at Urbana-Champaign). We also acknowledge financial support from the Spanish Comisión Asesora de Investigación Científica y Técnica (CAICYT) under Grant No. 789/84.

[1]R. Harris, M. Plischke, and M. J. Zuckermann, Phys. Rev. Lett. **31**, 160 (1973).
[2]J. M. D. Coey, J. Appl. Phys. **49**, 1646 (1978).
[3]J. J. Rhyne, J. H. Schelleng, and N. C. Koon, Phys. Rev. B **11**, 4672 (1974).
[4]L. S. Barton and M. B. Salamon, Phys. Rev. B **25**, 2030 (1982).
[5]S. Von Molnar, T. R. McGuire, R. J. Gambino, and B. Barbara, J. Appl. Phys. **53**, 7666 (1982); **53**, 2350 (1982).
[6]B. Dieny and B. Barbara, J. Phys. **46**, 293 (1985).
[7]B. Dieny and B. Barbara, Phys. Rev. Lett. **57**, 1169 (1986).
[8]D. J. Sellmyer and S. Nafis, Phys. Rev. Lett. **57**, 1173 (1986).
[9]D. J. Sellmyer and S. Nafis, J. Magn. Magn. Mater. **54–57**, 113 (1986).
[10]K. H. Fischer and A. Zippelius, Prog. Theor. Phys. Suppl. **87**, 165 (1986).
[11]A. del Moral, C. Cornelius, and B. D. Rainford (unpublished).
[12]Y. Imry and S. K. Ma, Phys. Rev. Lett. **35**, 1399 (1975).
[13]A. Aharony and E. Pytte, Phys. Rev. Lett. **45**, 1583 (1980).
[14]E. M. Chudnovsky, W. M. Saslow, and R. A. Serota, Phys. Rev. B **33**, 251 (1986).
[15]E. Callen, Y. J. Liu, and J. R. Cullen, Phys. Rev. B **16**, 263 (1977).
[16]J. D. Patterson, G. R. Gruzalski, and D. J. Sellmyer, Phys. Rev. B **18**, 1377 (1978).
[17]A. del Moral, J. I. Arnaudas, and K. A. Mohammed, Solid State Commun. **58**, 395 (1986).
[18]A. Aharony, Phys. Rev. B **12**, 1038 (1975).
[19]J. H. Chen and T. C. Lubensky, Phys. Rev. B **16**, 2106 (1977).
[20]A. Fert and I. A. Campbell, J. Phys. F **8**, L57 (1978).
[21]J. B. Bieri, J. Sanchez, A. Fert, D. Bertrand, and A. R. Fert, J. Appl. Phys. **53**, 2347 (1982).
[22]E. M. Chudnovsky and R. A. Serota, J. Phys. C **16**, 4181 (1983).
[23]R. W. Cochrane, R. Harris, and M. Plischke, J. Non-Cryst. Solids **15**, 239 (1974).
[24]D. Sherrington and S. Kirkpatrick, Phys. Rev. Lett. **35**, 1792 (1975).
[25]S. K. Ghatak and D. Sherrington, J. Phys. C **10**, 3149 (1977).
[26]S. F. Edwards and P. W. Anderson, J. Phys. F **5**, 965 (1975).
[27]S. Kirkpatrick and D. Sherrington, Phys. Rev. B **17**, 4384 (1978).
[28]S. Chikazumi, *Physics of Magnetism* (Wiley, New York, 1964), p. 161.
[29]C. M. Soukoulis and K. Levin, Phys. Rev. Lett. **39**, 581 (1977).
[30]C. M. Soukoulis and K. Levin, Phys. Rev. B **18**, 1439 (1978).
[31]E. W. Lee, in *Experimental Magnetism*, edited by G. M. Kalvius and R. S. Tebble (Wiley, New York, 1979), Vol. 1.
[32]M. R. Ibarra, Ph.D. thesis, University of Zaragoza, 1983.
[33]P. A. Algarabel, Ph.D. thesis, University of Zaragoza, 1986.
[34]M. T. Hutchings, Solid State Phys. **16**, 227 (1964).
[35]A. J. Freeman and R. E. Watson, Phys. Rev. **127**, 2058 (1962).
[36]A. del Moral and E. W. Lee, J. Phys. C **13**, 6219 (1980).
[38]Y. Suzuki and T. Egami, J. Magn. Magn. Mater. **31–34**, 1549 (1983).
[37]Y. Suzuki and T. Egami, J. Magn. Magn. Mater. **31–34**, 1549 (1983).
[38]N. J. Hunter (unpublished).